THE JOURNAL OF PHYSICAL CHEMISTRY Letters

Letter

pubs.acs.org/JPCL

Size Effect in the Ionization Energy of PAH Clusters

C. Joblin,*[,†] L. Dontot,[†] G. A. Garcia,[‡] F. Spiegelman,[¶] M. Rapacioli,[¶] L. Nahon,[‡] P. Parneix,[§] T. Pino,[§] and P. Bréchignac[§]

[†]IRAP, Université de Toulouse, CNRS, UPS, CNES, 9 Av. du Colonel Roche, 31028 Toulouse Cedex 4, France

[‡]Synchrotron SOLEIL, L'Orme des Merisiers, 91192 Gif sur Yvette Cedex, France

[¶]Laboratoire de Chimie et Physique Quantiques LCPQ/IRSAMC, Université de Toulouse (UPS) and CNRS, 118 Route de Narbonne, 31062 Toulouse, France

[§]Institut des Sciences Moléculaires d'Orsay, CNRS, Univ Paris Sud, Université Paris-Saclay, F-91405 Orsay, France

Supporting Information

ABSTRACT: We report the first experimental measurement of the near-threshold photoionization spectra of polycyclic aromatic hydrocarbon clusters made of pyrene $C_{16}H_{10}$ and coronene $C_{24}H_{12}$, obtained using imaging photoelectron−photoion coincidence spectrometry with a VUV synchrotron beamline. The experimental results of the ionization energy are compared to calculated ones obtained from simulations using dedicated electronic structure treatment for large ionized molecular clusters. Experiment and theory consistently find a decrease of the ionization energy with cluster size. The inclusion of temperature effects in the simulations leads to a lowering of this energy and to quantitative agreement with the experiment. In the case of pyrene, both theory and experiment show a discontinuity in the IE trend for the hexamer. This work demonstrates the ability of the models to describe the electronic structure of PAH clusters and suggests that these species are ionized in astronomical environments where they are thought to be present.

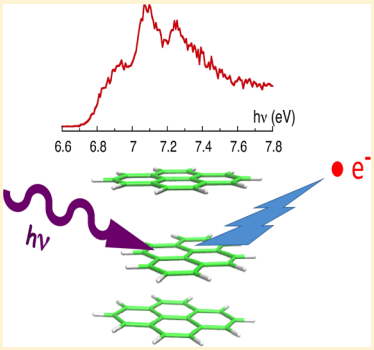

For almost 30 years, astronomers, physicists and chemists have striven to assess the astrophysical significance of interstellar polycyclic aromatic hydrocarbons (PAHs) (see ref 1 for a recent compilation of articles). The presence of these PAHs has been proposed to account for a set of aromatic infrared bands in the 3−15 μm range. These bands are observed in emission from interstellar and circumstellar regions that are exposed to ultraviolet stellar light, which are generally referred to as photodissociation regions (PDRs). However, the main drawback of the initial PAH hypothesis remains, that is, that no individual species have been identified so far. Still, the detection of C_{60} and C_{60}^+ through their infrared signatures has recently shown that large gas-phase aromatic molecules exist in PDRs.[2,3] Rather than looking for the spectral signatures of specific molecules, one could constrain the chemical scenarios that lead to the formation of these large carbonaceous molecules in space. In PDRs, the analysis of astronomical observations suggests that these species are produced by photoevaporation of nanograins, which molecular clusters could mimic.[4] A few studies have been performed to evaluate the formation and survival of neutral PAH clusters in PDRs.[5,6] Ionized PAH clusters have also been considered as species of astrophysical interest because their binding energies are expected to be larger than those of the corresponding neutrals, and therefore, they are expected to survive on a longer time scale in PDRs.[5,7] The astrophysical application has motivated experimental studies on the interaction of PAH and/or C_{60} clusters with UV laser photons ($h\nu$ = 4 eV)[8] and with fast ions beams.[9−12] In addition to the study of the induced fragmentation routes for such clusters, these works demonstrated the possibility for molecular growth inside the clusters. In the modeling studies mentioned above, the properties of PAH clusters have been simulated because quantitative data from experiments are still rather limited. Yet, describing the electronic structure of large clusters with up to a 1000 atoms remains a challenging task for theory. In addition, in the case of ionized clusters, one has to describe charge resonance, which constitutes another difficulty.[7] Therefore, experimental data are critical to benchmark models. In the present study, we report the first experimental measurement of spectral features accompanying the ionization onset of PAH clusters made of pyrene $C_{16}H_{10}$ and coronene $C_{24}H_{12}$, respectively. Calculations were performed to determine the vertical ionization potentials (IPv's) of the pertinent isomers. They were complemented by simulations at finite temperatures in order to include the contribution of thermally populated isomers. The results provide a valuable benchmark for a detailed critical comparison with experimental data, which, consequently, may validate the structural information produced by the model.

Experiments have been performed at the DESIRS VUV beamline[13] of the French synchrotron facility SOLEIL using the molecular beam setup available at the SAPHIRS permanent

Received: June 17, 2017
Accepted: July 25, 2017
Published: July 25, 2017

DOI: 10.1021/acs.jpclett.7b01546
J. Phys. Chem. Lett. 2017, 8, 3697−3702

endstation coupled to an imaging photoelectron−photoion coincidence (iPEPICO) spectrometry technique.[14] In brief, the PAH clusters are generated by supersonic expansion from a high-pressure argon reservoir containing the heated PAH sample. The resulting molecular beam crosses the VUV synchrotron beam. The produced cations are detected in coincidence with the photoelectrons that are analyzed in kinetic energy. Details can be found in the Experimental and Theoretical Methods section.

The mass spectrum displayed in Figure 1 presents the relative intensity distribution of the pyrene clusters that was

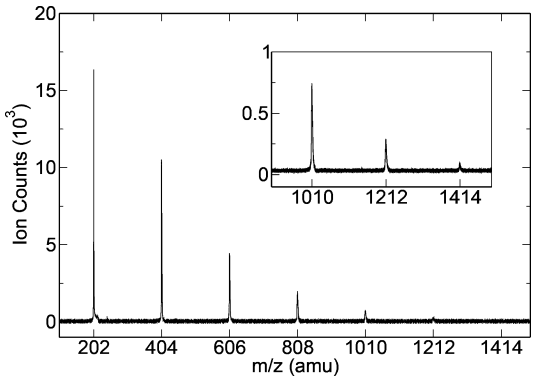

Figure 1. Mass spectrum showing the pyrene cluster distribution from the time-of-flight spectrometer integrated over all of the photon energies measured in one of the performed scans.

obtained in our experimental conditions. It demonstrates that they are observed up to the heptamer at m/z = 1414. Additionally, ion images obtained in the studied energy range show that no detectable fragmentation occurs in this range (see Figure S1 in the Supporting Information). In addition, the calculated energy needed for the evaporation of one monomer from the pyrene and coronene ionized clusters is between 0.8 and 1 eV.[7,15] Therefore, the onsets of ionization are not expected to be contaminated by dissociative ionization.

The mass-selected threshold photoelectron spectra (TPES) are shown in Figure 2 for both pyrene and coronene clusters up to an energy of 7.9 eV. When increasing the size of the clusters, both a broadening of the spectral features and a shift of the ionization onset toward lower energies are observed. The noise significantly increases for the largest clusters due to their low abundance. In the following, we specifically focus on the ionization energy (IE). Considering the complex shape of these yield curves, we chose to arbitrarily define the IE for each species as the lowest value of the photon energy for which the TPES signal reaches 10% of the value at the first inflection point, which we define as the local maximum. The evolution of the experimental IE values with cluster size is displayed in Figure 3 (trace in black). A decrease with cluster size is observed except for the pyrene hexamer.

To further discuss the IE features, we performed simulations to obtain theoretical values for the IE, taking into account temperature and isomer effects. The electronic structure of the clusters was described using self-consistent density functional based tight binding methodology (DFTB)[17] combined with a configuration interaction (CI; DFTB-CI) scheme to account for charge delocalization in the ions.[18,19] The most stable structures of the neutrals were searched through a global optimization process (Figure 4). The single-stack geometry that was already exemplified in a previous work on coronene[20] was obtained for the lowest sizes, albeit distorted with respect to perfect alignment. Moreover, multiple-stack structures become more favorable for the coronene pentamer (Figure S12), and for pyrene clusters larger than the trimer (Figures S5−S8). In the cationic state, the calculations show that the charge remains localized in a core consisting of 1−3 units (cf. Table 1). For a given size and isomer, we first calculate the IPv assuming the Franck−Condon approximation, that is, the energies of the cationic clusters are calculated at the neutral geometry (see Tables S1 and S2 in the Supporting Information). IPv values

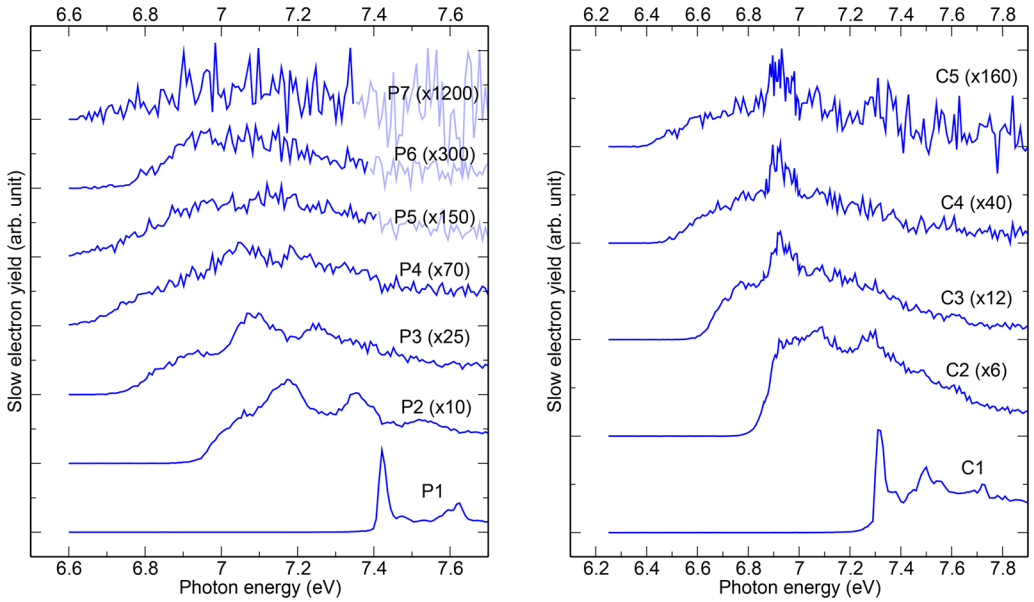

Figure 2. Mass-selected threshold photoelectron spectra (TPES) of the monomer and clusters of pyrene (P; left panel) and coronene (C; right panel); the labels $P_{i=1-7}$ and $C_{j=1-5}$ refer to the number of monomer units. The overall energy resolutions achieved were 30 and 15 meV for pyrene and coronene clusters, respectively.

DOI: 10.1021/acs.jpclett.7b01546
J. Phys. Chem. Lett. 2017, 8, 3697−3702

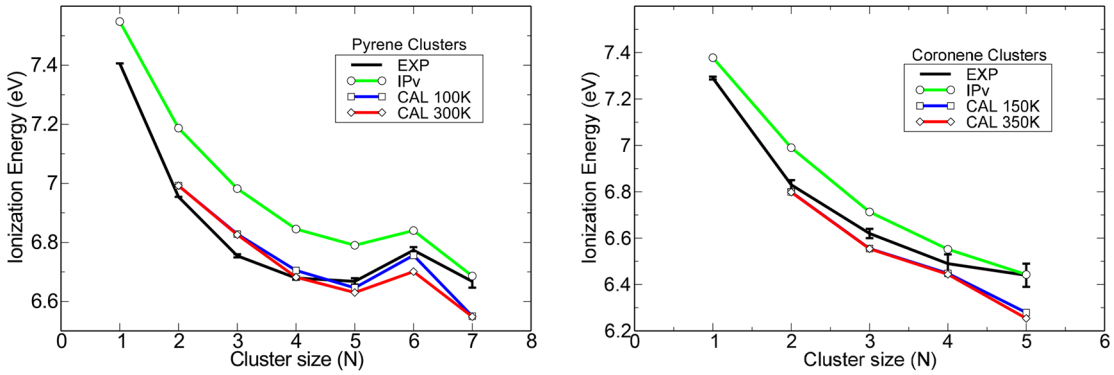

Figure 3. Evolution of the IE with cluster size for pyrene (left) and coronene (right) clusters. Experimental values are compared with IPv values of the lowest-energy isomers and theoretical IEs extracted at two finite temperatures. The values from the size scaling formula of Johansson et al.[16] are also shown. The 1σ experimental error bars only take into account the statistical error and are estimated assuming a Poisson distribution on the electron image pixels.

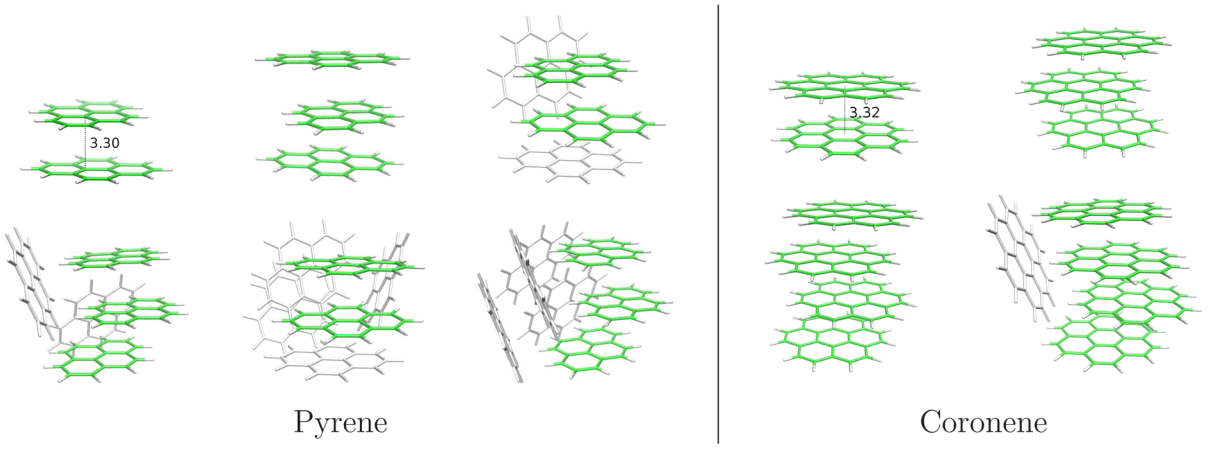

Figure 4. Lowest-energy structures for neutral pyrene (left panel) and coronene (right panel) clusters. In cationic states, molecules in green carry the charge, and molecules in gray are mostly neutral. The indicated distances are provided in Å.

Table 1. Charge Distribution over the PAH Units in Cluster Cations at the Geometries of the Corresponding Neutral Clusters

size (N)	$(C_{16}H_{10})_N^+$	$(C_{24}H_{12})_N^+$
2	50.0|50.0	50.0|50.0
3	67.2|16.4|16.4	60.4|19.7|19.7
4	56.4|36.3|7.3|0.1	39.4|39.4|10.6|10.6
5	68.0|16.0|16.0|0.0|0.0	57.9|32.5|4.9|3.2|1.4
6	69.6|23.5|5.6|1.0|0.2|0.1	
7	63.9|17.6|17.6|0.3|0.3|1.8|1.8	

were previously reported in the case of coronene for perfectly regular stack geometries,[7,16,21] but we report here the first values for globally optimized clusters. As shown in Figure 3, the theoretical IPv curve corresponding to the lowest-energy isomer for each size displays a general trend with decreasing values for increasing sizes, in very good agreement with the experimental behavior, but exhibits higher values with an overall shift of 0.1−0.2 eV. Thermal effects were then taken into account by combining a Boltzmann distribution scheme in order to weight the contributions from the different isomers and a Gaussian width to assume thermal broadening within each isomer basin (see the Experimental and Theoretical Methods section). This allowed us to generate theoretical ionization curves from which IE values could be extracted with the same procedure as that for the experimental curves (see above). The theoretical ionization curves as well as some relevant neutral isomers and their energetic properties are presented in the Supporting Information.

The theoretical IEs are found at values 0.1−0.2 eV below the IPv values of the lowest-energy isomers, which improves the match with the experimental data (cf. Figure 3). The difference observed between the two finite temperatures suggests, however, that the shift is generally less related to the isomer population than to the width of the Gaussian energy distribution with which each transition was convolved (see the Experimental and Theoretical Methods section and Supporting Information). Nevertheless, there are cases in which the low-energy isomers are quasi-degenerate with the lowest one and therefore significantly contribute to the spectrum. In the considered range of temperatures, a significant temperature effect is seen on the hexamer of pyrene with a shift close to −0.1 eV between 100 and 300 K. It is interesting to note that for both the hexamer (P6) and the heptamer (P7), only 4 isomers represent 95% of the thermal population at 100 K, whereas 22 isomers are involved at 300 K. The stronger temperature effect on P6 is related to the range of IPv values associated with these isomers (cf. Table S1 in the Supporting Information for IPv values of some relevant isomers). This range is much larger for P6. Values at 300 K (100 K) are 0.66 eV (0.22 eV) to be compared with 0.24 eV (0.09 eV) for P7.

DOI: 10.1021/acs.jpclett.7b01546
J. Phys. Chem. Lett. 2017, 8, 3697−3702

While the energies of the neutral isomers are quite close, the energies of the ions at those geometries may differ significantly. Theory can thus provide a possible explanation for the break in the trend observed in the IE for P6, in both the experimental and theoretical results, showing that, at the geometry of the neutral, this ion is less stable relative to its neighbors. This can be understood from the charge repartition analysis. In neutrals, the driving forces result from weak electrostatic and van der Waals interactions, while in cations charge delocalization and polarization forces are dominant, resulting in a larger binding energy in cations relative to neutrals. Considering adiabatic relaxation of the pyrene cluster cations, we obtain from DFTB-CI optimization a charge repartition of 0.5|0.5, 0.26|0.48|0.26, and 0.10|0.40|0.40|0.10 for the dimer, trimer, and tetramer cations, respectively. This shows that the charge delocalization extends significantly on dimers or trimers. At the geometries of neutral clusters, ion relaxation is not achieved and the charge delocalization is slightly smaller even though it is still found to be mostly delocalized over two (cases $N = 2, 4$) or three (cases $N = 3, 5, 6, 7$) molecules, as seen in Table 1. Also, except for the dimer, a larger charge is carried by a single molecule (cf. Table 1 and Figure 4). For the particular case of the P6 hexamer, the structure changes from a trimer core stack in the pentamer to a dimer core and back to a trimer core for the heptamer. In addition, the charge delocalization presents the strongest dissymmetry (0.7 of the charge carried by a single molecule). The combination of these features is likely at the origin of the larger IE for this size.

In the present comparison with experiment, we have assumed the Franck−Condon (vertical) approximation. The geometries considered are not the relaxed geometries of the ions, which require structural optimization with charge delocalization and polarization interactions. From the above-mentioned calculations on ion relaxation, we can get values for the adiabatic ionization potentials, IPa's, in the case of the dimer, trimer, and tetramer pyrene cations (cf. Table S1 in the Supporting Information). Due to relaxation effects, these values are found to be well below the IPv values and even below the experimental IE values. This supports the validity of the Franck−Condon approximation in the comparison with experiment. Finally, we would like to mention that remaining sources of uncertainties can be present in the calculations such as DFTB and DFTB-CI accuracy, as well as consequences of zero-point-energy and anharmonic effects not taken into account in the present work.

The present study reports the first experimental determination of the IEs of PAH clusters in the range of $N = 2−7$. The IEs are found to decrease with cluster size, with the exception of the pyrene hexamer. The consistency between experiment and theory gives support to the cluster geometries shown in Figure 4. While the decrease of the IEs is a general feature in clusters, the fine description of the size effects requires a model allowing the interplay between structural global optimization and electronic patterns for neutrals and cations as made possible with DFTB-based simulations. The temperature has been included in the simulations in the form of a Boltzmann isomer population to generate theoretical ionization spectra from which IE values could be derived consistently with the experiment. In future works, the model could also be used further beyond the ionization onset to calculate the electronic excited states[19] for the different cationic isomers. This will help disentangling in the recorded TPES spectra the part due to vibrations from that due to excited electronic state transitions in isomers (Figure 2). The model could also be extended to treat heterogeneous or larger PAH clusters.

Finally, a chemical scenario has been proposed based on analysis of astronomical observations in which UV photons penetrate a molecular cloud leading to the evaporation of very small grains (assumed to be PAH clusters) and the production of PAH molecules. Closer to the star and in more dilute regions, PAHs are observed to be mainly positively ionized.[22,23] Our study brings new information on the ionization state of astro-PAH clusters. Indeed, in the regions where they are thought to be observed, they absorb VUV photons at a typical energy of 6−7 eV[5] and with a higher photoionization cross section than PAH monomers because of the larger number of C atoms, that is, of active electrons.[24] In addition, in these regions, the electron density is significantly lower compared to the border of the cloud.[25] This strongly indicates that PAH clusters, if present, are ionized while evaporating, making it worth exploring their survival in these environments.

EXPERIMENTAL AND THEORETICAL METHODS

Due to the low vapor pressure of PAHs, an in-vacuum stainless steel oven specially designed to reach high temperatures (up to 500 °C) was built. Typically, 1.5 g of coronene (99% purity from Sigma-Aldrich) or pyrene (98% purity from Fluka) was introduced into the oven and working temperatures of 340−360 and 180 °C were used for coronene and pyrene, respectively. The PAH vapor was mixed and driven by an Ar flow and then expanded through a 50 μm nozzle; the backing pressure, 1.1−1.2 bar, was adjusted to maximize the production of PAH clusters. The maximum size obtained for coronene clusters (up to the pentamer) and pyrene clusters (up to the heptamer) resulted from our choice to maintain stable expansion conditions in the cluster source while scanning the photon energy. The free jet was skimmed through a 2 mm ID orifice and passed through the ionization zone while crossing the VUV synchrotron beam at a right angle at the center of the iPEPICO spectrometer. We used DELICIOUS 2[14] for the coronene experiments reported here and its upgraded version DELICIOUS 3[26] for the pyrene clusters. Briefly, DELICIOUS 2 consists of a velocity map imaging (VMI) analyzer coupled in coincidence to a Wiley−McLaren time-of-flight (WM-TOF) spectrometer, which is able to provide mass-filtered photoelectron or photoion images. The ion images were recorded at several photon energies only to ensure that the detected clusters had no measurable translational energy within the photon energy range presented in this work and thus do not originate from a dissociative ionization event but rather from direct ionization of the neutral counterpart. DELICIOUS 3 has the ability to provide photoelectron and photoion images simultaneously, which means that on top of the mass selection ion translational energy selection is performed, again to consider only the parent ions and discard any possible fragments. Because not all of the capabilities of the newer spectrometer were used, the only real difference between both sets of experiments is the improved mass resolution for the pyrene runs, which did not affect the relative quality of the results. In all of the experiments, the electrostatic configuration was set as to ensure full transmission for all ions and electrons. The decrease of signal for increasing cluster size observed in Figure 1 is only attributed to the clusters relative abundance in the molecular beam and to the efficiency decrease of the microchannel plate ion detectors, estimated at 30% between 300 and 1500 amu. The cation spectroscopy was recorded with

DOI: 10.1021/acs.jpclett.7b01546
J. Phys. Chem. Lett. 2017, 8, 3697−3702

the threshold photoelectron technique by scanning the photon energy and taking into account only the slow electrons (<30 meV for coronene and <50 meV for pyrene clusters) for which the absolute VMI resolution is best, as previously described.[27]

Concerning the theoretical approach, the electronic structure of the clusters and potential energy surfaces are computed using self-consistent DFTB methodology[17] with dispersion corrections.[28] In order to ensure a proper description of the charge delocalization in ionized clusters, we used a scheme combining valence bond-type CI and constrained DFTB.[18,19] For neutrals, structural optimization was performed using a global search algorithm. Parallel-tempering Monte Carlo (MC) simulations[29] involving configurational exchanges between temperature-adjacent trajectories were first conducted in the rigid molecule approximation to sample low-energy configurations. Each of these configurations was then further optimized via a conjugated gradient scheme within an all-atom relaxation (namely intra- and intermolecular degrees of freedom).

At finite temperatures, IPv values were determined for the p isomers of interest and a theoretical ionization spectrum (IS) was built by assigning to each isomer (i) a Gaussian energy distribution associated with the entropic motion within its potential energy surface basin and (ii) a Boltzmann weight with respect to its energy ΔE_i above the most stable isomer. This led to

$$\mathrm{IS}(E) = A \sum_{i=1}^{\mathrm{p}} \exp\left[-\frac{\Delta E_i}{kT}\right] \exp\left[-\frac{(E - \mathrm{IPv}_i)^2}{2\sigma^2}\right] \quad (1)$$

where A is a normalization factor and σ the standard deviation of the Gaussian related to the FWHM. The latter was set to 0.15 eV for pyrene and 0.2 eV for coronene, estimated from MC simulations on the dimer species. Theoretical IE values can be extracted from the simulated spectra using the same 10% level procedure as that performed for the experimental data. This scheme was repeated at T = 100 and 300 K for pyrene clusters and at T = 150 and 350 K for coronene clusters. These values encompass the range of temperatures expected for the clusters in the experiment. Note that we have previously determined a typical vibrational temperature of 200 K for the coronene monomer in the molecular beam.[30]

■ ASSOCIATED CONTENT

Supporting Information

The Supporting Information is available free of charge on the ACS Publications website at DOI: 10.1021/acs.jpclett.7b01546.

Discussion of the dissociative ionization, theoretical ionization spectra for finite temperatures, and computed energetics and structural properties of PAH clusters (PDF)

■ AUTHOR INFORMATION

Corresponding Author

*E-mail: christine.joblin@irap.omp.eu.

ORCID

C. Joblin: 0000-0003-1561-6118

Notes

The authors declare no competing financial interest.

■ ACKNOWLEDGMENTS

We acknowledge the financial support of the Agence Nationale de la Recherche through the GASPARIM project Gas-phase PAH research for the interstellar medium (ANR-10-BLAN-0501) and computing ressources by the CALMIP supercomputing center (allocation 2015-P0059). L.D. thanks the ERC for support under Grant ERC-2013- Syg-610256-NANOCOSMOS.

■ REFERENCES

(1) Joblin, C., Tielens, A. G. G. M, Eds. *PAHs and the Universe: A Symposium to Celebrate the 25th Anniversary of the PAH Hypothesis*; EAS Publications Series; 2011; Vol. *46*.

(2) Sellgren, K.; Werner, M. W.; Ingalls, J. G.; Smith, J. D. T.; Carleton, T. M.; Joblin, C. C_{60} in Reflection Nebulae. *Astrophys. J., Lett.* **2010**, *722*, L54−L57.

(3) Berné, O.; Mulas, G.; Joblin, C. Interstellar C_{60}^+. *Astron. Astrophys.* **2013**, *550*, L4.

(4) Rapacioli, M.; Joblin, C.; Boissel, P. Spectroscopy of polycyclic aromatic hydrocarbons and very small grains in photodissociation regions. *Astron. Astrophys.* **2005**, *429*, 193−204.

(5) Rapacioli, M.; Calvo, F.; Joblin, C.; Parneix, P.; Toublanc, D.; Spiegelman, F. Formation and destruction of polycyclic aromatic hydrocarbon clusters in the interstellar medium. *Astron. Astrophys.* **2006**, *460*, 519−531.

(6) Montillaud, J.; Joblin, C. Absolute evaporation rates of non-rotating neutral polycyclic aromatic hydrocarbon clusters. *Astron. Astrophys.* **2014**, *567*, A45.

(7) Rapacioli, M.; Spiegelman, F. Modelling singly ionized coronene clusters. *Eur. Phys. J. D* **2009**, *52*, 55−58.

(8) Bréchignac, P.; Schmidt, M.; Masson, A.; Pino, T.; Parneix, P.; Bréchignac, C. Photoinduced products from cold coronene clusters. A route to hydrocarbonated nanograins? *Astron. Astrophys.* **2005**, *442*, 239−247.

(9) Holm, A. I. S.; Zettergren, H.; Johansson, H. A. B.; Seitz, F.; Rosén, S.; Schmidt, H. T.; Ławicki, A.; Rangama, J.; Rousseau, P.; Capron, M.; et al. Ions Colliding with Cold Polycyclic Aromatic Hydrocarbon Clusters. *Phys. Rev. Lett.* **2010**, *105*, 213401.

(10) Zettergren, H.; Rousseau, P.; Wang, Y.; Seitz, F.; Chen, T.; Gatchell, M.; Alexander, J. D.; Stockett, M. H.; Rangama, J.; Chesnel, J. Y.; et al. Formations of Dumbbell C_{118} and C_{119} inside Clusters of C_{60} Molecules by Collision with α Particles. *Phys. Rev. Lett.* **2013**, *110*, 185501.

(11) Gatchell, M.; Rousseau, P.; Domaracka, A.; Stockett, M. H.; Chen, T.; Schmidt, H. T.; Chesnel, J. Y.; Méry, A.; Maclot, S.; Adoui, L.; et al. Ions colliding with mixed clusters of C_{60} and coronene: Fragmentation and bond formation. *Phys. Rev. A: At., Mol., Opt. Phys.* **2014**, *90*, 022713.

(12) Delaunay, R.; Gatchell, M.; Rousseau, P.; Domaracka, A.; Maclot, S.; Wang, Y.; Stockett, M. H.; Chen, T.; Adoui, L.; Alcamí, M.; et al. Molecular Growth Inside of Polycyclic Aromatic Hydrocarbon Clusters Induced by Ion Collisions. *J. Phys. Chem. Lett.* **2015**, *6*, 1536−1542.

(13) Nahon, L.; de Oliveira, N.; Garcia, G. A.; Gil, J.-F.; Pilette, B.; Marcouillé, O.; Lagarde, B.; Polack, F. DESIRS: a state-of-the-art VUV beamline featuring high resolution and variable polarization for spectroscopy and dichroism at SOLEIL. *J. Synchrotron Radiat.* **2012**, *19*, 508−520.

(14) Garcia, G. A.; Soldi-Lose, H.; Nahon, L. A versatile electron-ion coincidence spectrometer for photoelectron momentum imaging and threshold spectroscopy on mass selected ions using synchrotron radiation. *Rev. Sci. Instrum.* **2009**, *80*, 023102.

(15) Dontot, L. *Propriétés structurales et spectroscopiques des agrégats dahydrocarbures aromatiques polycycliques*. Ph.D. thesis, Université de Toulouse (UPS), 2014.

(16) Johansson, H. A. B.; Zettergren, H.; Holm, A. I. S.; Seitz, F.; Schmidt, H. T.; Rousseau, P.; Ławicki, A.; Capron, M.; Domaracka, A.; Lattouf, E.; et al. Ionization and fragmentation of polycyclic aromatic hydrocarbon clusters in collisions with keV ions. *Phys. Rev. A: At., Mol., Opt. Phys.* **2011**, *84*, 043201.

DOI: 10.1021/acs.jpclett.7b01546
J. Phys. Chem. Lett. 2017, 8, 3697−3702

(17) Elstner, M.; Porezag, D.; Jungnickel, G.; Elsner, J.; Haugk, M.; Frauenheim, T.; Suhai, S.; Seifert, G. Self-consistent-charge density-functional tight-binding method for simulations of complex materials properties. *Phys. Rev. B: Condens. Matter Mater. Phys.* **1998**, *58*, 7260−7268.
(18) Rapacioli, M.; Spiegelman, F.; Scemama, A.; Mirtschink, A. Modeling Charge Resonance in Cationic Molecular Clusters: Combining DFT-Tight Binding with Configuration Interaction. *J. Chem. Theory Comput.* **2011**, *7*, 44−55.
(19) Dontot, L.; Suaud, N.; Rapacioli, M.; Spiegelman, F. An extended DFTB-CI model for charge-transfer excited states in cationic molecular clusters: model studies versus ab initio calculations in small PAH clusters. *Phys. Chem. Chem. Phys.* **2016**, *18*, 3545−3557.
(20) Rapacioli, M.; Calvo, F.; Spiegelman, F.; Joblin, C.; Wales, D. J. Stacked Clusters of Polycyclic Aromatic Hydrocarbon Molecules. *J. Phys. Chem. A* **2005**, *109*, 2487−2497.
(21) Rapacioli, M.; Simon, A.; Dontot, L.; Spiegelman, F. Extensions of DFTB to investigate molecular complexes and clusters. *Phys. Status Solidi B* **2012**, *249*, 245−258.
(22) Berné, O.; Joblin, C.; Deville, Y.; Smith, J. D.; Rapacioli, M.; Bernard, J. P.; Thomas, J.; Reach, W.; Abergel, A. Analysis of the emission of very small dust particles from Spitzer spectro-imagery data using blind signal separation methods. *Astron. Astrophys.* **2007**, *469*, 575−586.
(23) Pilleri, P.; Montillaud, J.; Berné, O.; Joblin, C. Evaporating very small grains as tracers of the UV radiation field in photo-dissociation regions. *Astron. Astrophys.* **2012**, *542*, A69.
(24) Douix, S.; Duflot, D.; Cubaynes, D.; Bizau, J.-M.; Giuliani, A. Photoionization of the Buckminsterfullerene Cation. *J. Phys. Chem. Lett.* **2017**, *8*, 7−12.
(25) Montillaud, J.; Joblin, C.; Toublanc, D. Evolution of polycyclic aromatic hydrocarbons in photodissociation regions. Hydrogenation and charge states. *Astron. Astrophys.* **2013**, *552*, A15.
(26) Garcia, G. A.; Cunha de Miranda, B. K.; Tia, M.; Daly, S.; Nahon, L. DELICIOUS III: A multipurpose double imaging particle coincidence spectrometer for gas phase vacuum ultraviolet photo-dynamics studies. *Rev. Sci. Instrum.* **2013**, *84*, 053112.
(27) Poully, J. C.; Schermann, J. P.; Nieuwjaer, N.; Lecomte, F.; Gregoire, G.; Desfrancois, C.; Garcia, G. A.; Nahon, L.; Nandi, D.; Poisson, L.; et al. Photoionization of 2-pyridone and 2-hydroxypyridine. *Phys. Chem. Chem. Phys.* **2010**, *12*, 3566−3572.
(28) Rapacioli, M.; Spiegelman, F.; Talbi, D.; Mineva, T.; Goursot, A.; Heine, T.; Seifert, G. Correction for dispersion and Coulombic interactions in molecular clusters with density functional derived methods: Application to polycyclic aromatic hydrocarbon clusters. *J. Chem. Phys.* **2009**, *130*, 244304.
(29) Calvo, F. All-exchanges parallel tempering. *J. Chem. Phys.* **2005**, *123*, 124106.
(30) Bréchignac, P.; Garcia, G. A.; Falvo, C.; Joblin, C.; Kokkin, D.; Bonnamy, A.; Parneix, P.; Pino, T.; Pirali, O.; Mulas, G.; et al. Photoionization of cold gas phase coronene and its clusters: Autoionization resonances in monomer, dimer, and trimer and electronic structure of monomer cation. *J. Chem. Phys.* **2014**, *141*, 164325.

DOI: 10.1021/acs.jpclett.7b01546
J. Phys. Chem. Lett. 2017, 8, 3697−3702